Linear response theoretical study of the exchange interactions in Mn-doped ScN: Effects of disorder, band gap, and doping

Aditi Herwadkar,[1,2] Walter R. L. Lambrecht,[1] and Mark van Schilfgaarde[3]
[1]*Department of Physics, Case Western Reserve University, Cleveland, Ohio 44106-7079, USA*
[2]*Department of Physics and Astronomy, University of Nebraska, Lincoln, Nebraska 68588-0111, USA*
[3]*School of Materials, Arizona State University, Tempe, Arizona 85287, USA*
(Received 17 December 2007; published 17 April 2008)

Linear response calculations of the magnetic exchange interactions in Mn-doped ScN were carried out in the rigid-spin approximation by using the muffin-tin-orbital Green's function method. They show that the exchange interactions are long range and strongly affected by disorder, band gap corrections, and doping. The cluster variation method is shown to reduce the T_c by about 30% as compared to the mean-field treatment. A Curie temperature saturating with Mn concentration above 20% at ~440 K is predicted with a semiconducting behavior present until about 15%. Both *p*- and *n*-type doping are found to decrease T_c.

DOI: 10.1103/PhysRevB.77.134433 PACS number(s): 75.50.Pp, 71.55.Eq, 75.30.Et, 85.75.−d

I. INTRODUCTION

The recent interest in semiconductor based spin-dependent electronics has created a need for high-Curie-temperature dilute magnetic semiconductors (DMSs). Traditional zinc blende structure semiconductors suffer from a low solubility typical of magnetic impurity atoms, such as transition metal ions, which manifests itself in the occurrence of secondary phases with a crystal structure different from the host. To prevent this, one usually resorts to nonequilibrium growth techniques with less than optimal temperatures for crystalline quality. As an alternative, we investigate the rock-salt structure semiconductor ScN, because it shares its crystal structure with magnetic (or antiferromagnetic) transition metal nitrides.[1] Mixed alloys of $Mn_xSc_{1-x}N$ have already been shown to be feasible by molecular beam epitaxy growth up to $x \approx 0.26$,[2] but systematic magnetic studies of them have not yet been reported.[3]

In a previous study,[1] the exchange interactions were estimated by using a direct supercell approach, in which the total energies of near-neighbor pairs of parallel or antiparallel Mn spins are fitted to a Heisenberg Hamiltonian. This commonly used approach makes the crucial (but erroneous) assumption that the interactions are relatively short range so that interactions with distant cells can be neglected. In this paper, we revisit the problem of the exchange interactions in Mn-doped ScN by using a linear response approach developed by Liechtenstein *et al.*[4,5] The method is formulated within spin density functional theory[6–8] and the calculations are all carried out in the atomic-sphere approximation (ASA) of the linearized muffin-tin-orbital (LMTO) method.[9]

After showing consistency of the present approach with our earlier results for the sum of exchange interactions but not the individual ones, we turn to the study of disorder effects in large unit cells. We find that the exchange interactions are long range, and strongly influenced by disorder, as also observed in other DMSs.[10,11] Including a gap correction is found to strongly affect the nature of the interactions beyond about 10 Å. We study the T_c as a function of Mn concentration by using a cluster variation method (CVM), as recently generalized to a classical Heisenberg Hamiltonian by Samolyuk and Antropov[12] and shown to provide accurate estimates of T_c for DMS by a comparison to spin dynamics simulations.[10] Finally, we study doping effects by additional free carriers.

II. COMPUTATIONAL METHOD

The calculations are performed by using the linear response approach of Liechtenstein *et al.*[4,5] within the ASA of the LMTO method.[9] The former is based on three main points: First, the Andersen force theorem, which allows one to calculate the total energy change as a change in only the sum of the one-electron energies upon rotation of the spin direction of frozen potentials,

$$\delta E = \sum_i^{occ} \delta\epsilon_i = \int_0^{\epsilon_F} \epsilon \delta D(\epsilon) d\epsilon, \tag{1}$$

where $\delta D(\epsilon)$ is the change in density of states. Second, charge neutrality of this rotation, which allows one to use a partial integration,

$$\int_0^{\epsilon_F} \epsilon \delta D(\epsilon) d\epsilon = -\int_0^{\epsilon_F} N(\epsilon) d\epsilon, \tag{2}$$

with $\delta N(\epsilon)$ the change in integrated density of states. Third, the latter can be evaluated by the Lloyd phase shift formula[16] of multiple scattering theory. In the LMTO context, this is written as

$$\delta N(\epsilon) = \frac{1}{\pi} \mathrm{Im\ Tr\ ln}[1 + \delta \mathbf{P}(\epsilon)\mathbf{g}(\epsilon)]. \tag{3}$$

By using this formalism, one can calculate the change in energy corresponding to the rotation of a spin at i and j by $\pm\theta/2$ in closed form and, by identifying $\delta E_{ij} - \delta E_i - \delta E_j = J_{ij}\theta^2/4$, one obtains a closed expression for the exchange interactions,[4]

$$J_{ij} = \frac{2}{\pi}\int_0^{\epsilon_F} d\epsilon \,\mathrm{Im}\,\mathrm{Tr}\{\delta P_i g_{ij}^{\uparrow}\delta P_j g_{ij}^{\downarrow}\}, \tag{4}$$

where $\delta P_i = (P_i^{\uparrow} - P_i^{\downarrow})/2$, P_i are the LMTO potential functions, which correspond to the inverse t-matrix element in multiple scattering theory, and $\mathbf{g}(\epsilon) = [\mathbf{P}(\epsilon)\delta_{ij} - \mathbf{S}]^{-1}$ is the Green's function, with $\mathbf{S}$ the structure constants. Boldface indicates the matrix structure in the atomic sites, angular momenta, and spin. The calculations are performed in a system with periodic boundary conditions and, hence, one obtains $J_{ij}(\mathbf{k})$ with i,j inside the unit cell, in terms of the Green's functions $g_{ij}(\epsilon,\mathbf{k})$. By an inverse Fourier transformation, we obtain the real space $J_{i,j+\mathbf{T}}$, where $\mathbf{T}$ are lattice translation vectors. If we use an $N\times N\times N$ k-point mesh in the Brillouin zone, we obtain exchange interactions up to Nth neighbor cells. It is important to note that these are all obtained from the Green's function of the reference system without the need to calculate different magnetic configurations explicitly.

To simulate disordered systems, we follow the special quasirandom structure (SQS) approach proposed by Zunger *et al.*[17] in an implementation by Ruban *et al.*[18]

To calculate critical temperatures, we use both the mean-field (MF) approach and a cluster variation method as recently developed for the classical Heisenberg Hamiltonian.[12] The method is briefly described here for the sake of completeness. A general description of the cluster expansion approach can be found in Ref. 13. In the treatment of the Heisenberg Hamiltonian used here, only points and pairs are included in the cluster expansion. The free energy is expressed as

$$F = \sum_i F_i + \frac{1}{2}\sum_{ij}(F_{ij} - F_i - F_j), \tag{5}$$

with each "cluster" free energy F_i and F_{ij} given as

$$F_i = -T\ln Z_i = -T\ln \mathrm{Tr}\exp(-\beta H_i),$$

$$F_{ij} = -T\ln Z_{ij} = -T\ln \mathrm{Tr}\exp(-\beta H_{ij}). \tag{6}$$

They give the distribution of point and pair configurations as $\rho_i = \exp[\beta(F_i - H_i)]$, $\rho_{ij} = \exp[\beta(F_{ij} - H_{ij})]$. Here, Z_i, Z_{ij} are partition functions, $\beta = 1/k_B T$, the trace involves integration over all spin orientations, and H_i, H_{ij} are effective Hamiltonians for points and pairs, which are given in terms of renormalization fields ψ_i^j, ψ_i^{jj} describing their interaction with the environment,

$$H_i = -(\psi_i^j + \mu_B B m_i)e_i^z,$$

$$H_{ij} = -J_{ij}\mathbf{e}_i\cdot\mathbf{e}_j - (\psi_i^{jj} + \mu_B B m_i)e_i^z - (\psi_j^{jj} + \mu_B B m_j)e_j^z. \tag{7}$$

Spin waves are neglected and only the z component of the renormalizing fields is kept, where z is the direction of the external magnetic field B, $\mathbf{m}_i$ is the magnetic moment on the ith site, and $\mathbf{e}_i = \mathbf{m}_i/m_i$. These approximations are justified for temperatures higher than about $0.5T_c$. The equality of the expressions for the average magnetic moments $\mu_i = \langle e_i^z\rangle$ on each site as derivatives of the cluster free energy versus its corresponding renormalization field,

$$\mu_i = (\partial F_i/\partial\psi_i^j)_T,$$

$$\mu_i = (\partial F_{ij}/\partial\psi_i^{jj})_{T,J_{ij}}, \tag{8}$$

and the relation between the different types of cluster fields,

$$\sum_j (\psi_i^{jj} - \psi_i^j) + \psi_i^j = 0, \tag{9}$$

lead to a complete set of nonlinear equations for the magnetic moments and fields, which is solved by the Newton method, and allow one to evaluate the free energy as a function of temperature and external magnetic field. Hence, the magnetization can be obtained as a function of temperature, and the critical temperature T_c can be determined. A key point in the approach of Samolyuk and Antropov[12] is that evaluating the pair partition function as an integral over spin directions can be reduced to a sum over modified spherical Bessel functions following an approach previously presented by Stanley,[14]

$$Z_{ij} = \sum_{l=0}^{\infty}(2l+1)i_l(\beta h_i^{ij})i_l(\beta J_{ij})i_l(\beta h_j^{ij}), \tag{10}$$

where $h_i^{ij} = \psi_i^{ij} + \mu_B B m_i$ and $i_l(z) = \sqrt{\pi/(2z)}I_{l+1/2}(z)$, with $I_n(z)$ the modified Bessel function of the first kind.[19] The point partition function meanwhile is given by

$$Z_i = \sinh(\beta h_i)/(\beta h_i) = i_0(\beta h_i), \tag{11}$$

where $h_i = \psi_i^j + \mu_B B m_i$. It is important to keep in mind that this approach includes as distant pair interactions as are found to be important from the evaluation of the Heisenberg Hamiltonian. In a slightly different formulation, one can treat the weaker longer range interactions in mean field.[12] For our present purposes, we note that the method gave excellent agreement with spin-dynamics simulations for a very similar system of Mn-doped GaAs and Mn-doped GaN.[10]

III. RESULTS

A. Justification of approach

We start our study by examining the relative accuracy of collinear and noncollinear calculations of the exchange interactions. We consider a nearest-neighbor pair of Mn in ScN and calculate the energy change upon rotating the angle between their magnetic moments by θ. This calculation is performed in a 64 atom supercell by using the noncollinear ASA-LMTO band structure approach. This is done in the rigid-spin approximation,[5] in which the spin density has a constant direction in each sphere but the spin direction can vary from sphere to sphere.

The results are shown in the inset of Fig. 1. We note that the energy difference for a 180° rotation is 0.34 eV, which is in good agreement with our previous full potential LMTO calculation.[1] This shows that the neglect of atomic relaxations in our present ASA study is not important. However, we also see that the slope near the origin is smaller than that of the $J_1(1-\cos\theta)/2$ law predicted by the Heisenberg Hamiltonian.[15] If one defines the exchange interactions in

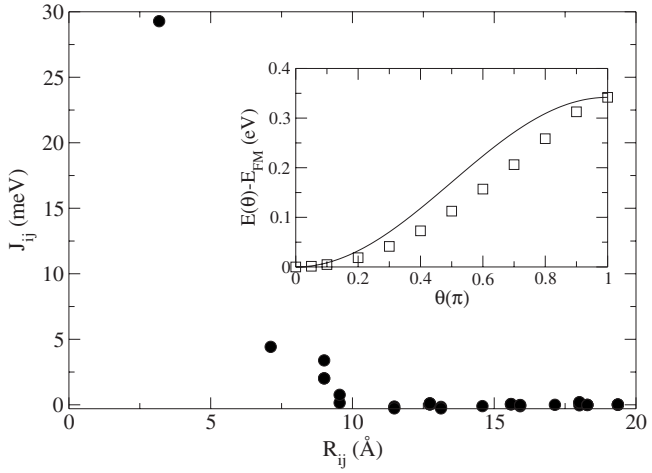

FIG. 1. Exchange interactions as function of distance in a periodic system of Mn-Mn nearest-neighbor pairs in a 64 atom supercell. Inset: Energy of a nearest-neighbor Mn pair relative to the ferromagnetic state as a function of rotation angle θ. The solid line indicates the $J_1(1-\cos\theta)$ law predicted by the classical Heisenberg Hamiltonian with nearest-neighbor interaction J_1 fixed by $E_{AF}-E_{FM}=2J_1$.

terms of the small angle deviations from the ferromagnetic reference state, then the energy change upon rotating the spin at the origin $\delta E_0 \approx J_0\theta^2/2$ with $J_0=\Sigma_j J_{0j}$, i.e., the sum of all exchange interactions connected to the atom at the origin. By assuming that interactions with neighboring cells were negligible, we would have identified J_0 with the nearest-neighbor exchange interaction J_{01}. The value obtained is $J_0=0.11$ eV, which is 35% smaller than the collinear result ($J_0=0.17$ eV).

Next, we consider the same 64 atom cell again but now calculate the exchange interactions by using the linear response approach[4,5] according to Eq. (4). The results for the same 64 atom cell with nearest-neighbor pair of Mn are shown in the main part of Fig. 1 as a function of distance R_{ij} between Mn atoms. While the nearest-neighbor interaction J_{01} is only about 30 meV, the sum $J_0=\Sigma_j J_{0j}\approx 0.14$ eV. Thus, the results agree closely with the previous calculation in terms of J_0, but the interpretation is totally different. We recognize now that the interactions are quite long ranged and the J_0, which we previously interpreted as the nearest-neighbor interaction, is in truth the *sum over many small long-range interactions*.

B. Exchange interactions

Next, we consider the effects of randomness by constructing 128 atom supercells with various concentrations of randomly placed Mn atoms. In fact, we pick for these random cells, so-called special quasirandom structures,[17,18] which are, in principle, optimized in their correlation functions such that a single structure can give an ensemble average of properties that converge rapidly enough in a cluster expansion.

In the top panel of Fig. 2 we show the local density approximation (LDA) results for the exchange interactions as a function of distance R_{ij}, multiplied by $(R_{ij}/a)^3$ so as to emphasize their long-range algebraic decay. Several conclusions can be drawn. First, the exchange interactions are not simply a function of distance. Different values are found for different pairs at the same distance. Secondly, up to about $R_{ij}/a \approx 2$, the interactions are predominantly positive, then they become predominantly negative until about $R_{ij}/a \approx 4$, and then become positive again. Together with the R_{ij}^{-3} decay, this suggests Ruderman–Kittel–Kasuya–Yosida (RKKY) behavior.[20–22] This is not surprising because in LDA, ScN has a zero band gap and the Mn-induced states form a metallic resonance overlapping with the host conduction band. From an analysis of the partial density of states (PDOS),[1] we learn that the $t_{2g\uparrow}$ (majority) states are filled with three electrons and lead to localized $S=3/2$ spins. The remaining electron per Mn (three are used to satisfy the bonding in the trivalent state) are spread over Mn $de_{g\uparrow}$ and $t_{2g\downarrow}$ and Sc dt_{2g} like bands. This is consistent with the magnetic moments, which vary from 2 to 3.5μ_B. Thus, we have diluted magnetic spins in an electron gas. By assuming the RKKY $\cos 2k_F r$ behav-

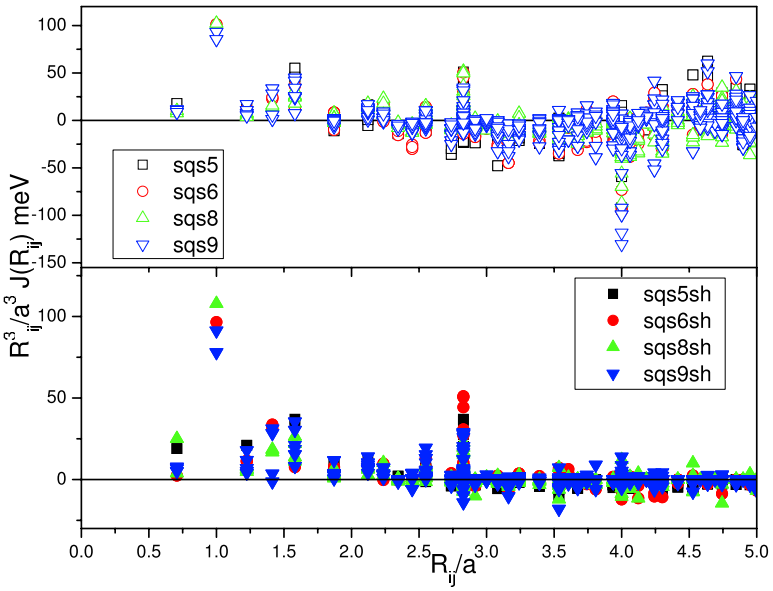

FIG. 2. (Color online) Exchange interactions in various 256 atom SQS cells with different concentrations of Mn (indicated by the number for each symbol) in ScN as a function of distance: top, LDA approximation; bottom, including gap correction.

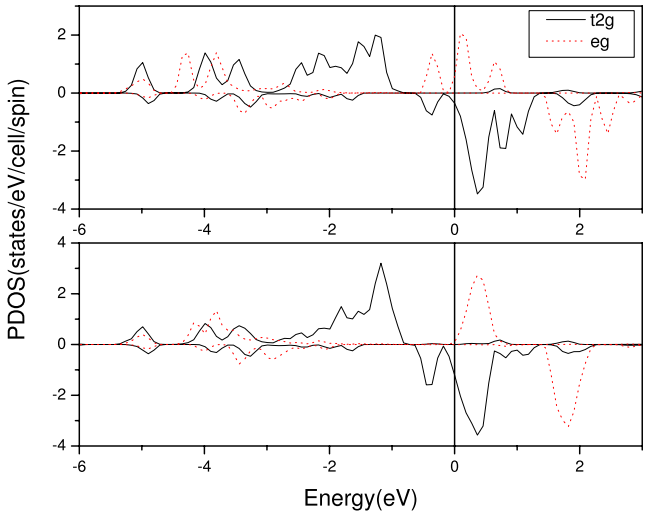

FIG. 3. (Color online) Mn d partial density of states on a Mn atom that has a second nearest-neighbor Mn (top) and on a Mn atom that does not have a second nearest-neighbor Mn (bottom).

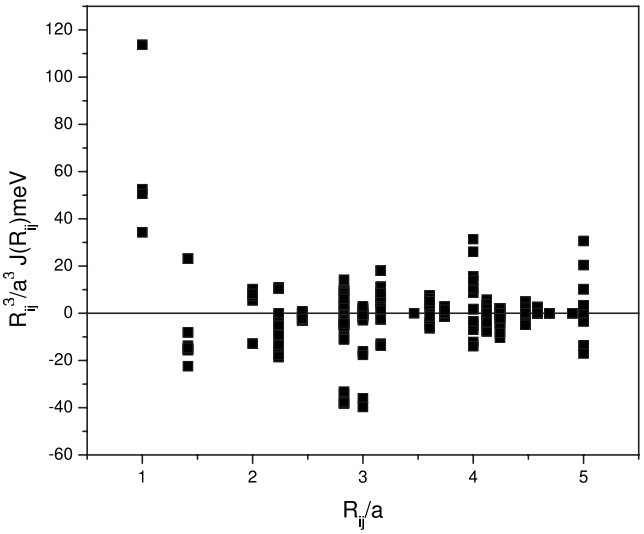

FIG. 4. Exchange interactions in a supercell of 8% Mn containing only second nearest-neighbor Mn pairs clustered together.

ior, and $k_F^3/3\pi^2=n$, the observed oscillations correspond to a free-electron carrier density of about $2\times10^{19}\ e/\mathrm{cm}^3$, which seems reasonable for a Mn-doping concentration of the order of a few percent.

To study whether ScN:Mn will behave as a DMS, it appears essential to take the band gap in ScN into account. In the LMTO method, we can correct the band gap underestimate by adding a rigid shift of the Sc d orbital energy.[23] While this was found to have only minor effects on magnetic moments and PDOS,[1] the J_{ij} are found to depend more subtly on this correction. As seen in the bottom panel of Fig. 2, the oscillations disappear when adding a gap shift and the long-range interactions are strongly reduced. This can be explained by the fact that there is now a weaker overlap of the Mn d $t_{2g\downarrow}$ band with the Sc d conduction band and, hence, fewer free carriers, thus reducing k_F. The electrons become trapped into Mn d impurity bands, which leads to a less effective coupling between atoms at distances larger than about three lattice constants.

Third, we can see a rather strong second nearest interaction, which indicates the occurrence of e_g-orbital mediated double exchange interactions via the intervening N, which is characteristic of the rocksalt structure. We find that the atoms with highest magnetic moments correspond to second nearest-neighbor pairs and have distinct looking PDOS. This is shown in Fig. 3. As can be seen in the top part, for a Mn which has a second nearest-neighbor Mn, an e_g majority spin band occurs below E_F and leads to a high spin state, effectively a magnetic moment $m>3\mu_B$, while for a Mn, which lacks such a neighbor, instead, the t_{2g} minority spin band is partially occupied, leading to a low spin state of about $2\mu_B$. These pairs have a slightly lower energy than other pairs, as was already discussed in our previous study.[1] Although their energy is higher than two separate Mn atoms, it shows a slight preference for second nearest-neighbor clusters. This gives rise to local pairs with strong ferromagnetic coupling and a large effective moment of about $6\mu_B$, which is embedded in the rest of the system.

To further study the effect of second nearest-neighbor pairs, we constructed a cell with 8% Mn, in which each Mn is part of a second nearest-neighbor pair, rather than following a random distribution. The results for the exchange interactions are shown in Fig. 4. It shows that a significant number of the interactions beyond second nearest neighbors are now antiferromagnetic and spoil the effect of the large second nearest-neighbor ferromagnetic interactions. This is disappointing but it is probably related to the fact that, in this particular cell, Mn is effectively segregated as a Mn-rich cluster, as can be seen in Fig. 5. It is consistent with MnN being antiferromagnetic.

C. Critical temperature

By averaging $J_i=\Sigma_j J_{ij}$ over the various atoms in the cell, $\bar{J}=N^{-1}\Sigma_i J_i$, we can obtain a mean-field approximation to $T_c \approx \bar{J}/3k_B$. A better estimate of T_c is obtained in the cluster variation method.[12] We note that, here, we do not pursue the very dilute limit where percolation effects could be dominant. Also, the exchange interactions are sizable up to at least fourth neighbors. Thus, we can trust our results down to the concentrations of a few percent. Both estimates of T_c are plotted in Fig. 6 with and without gap corrections. We see that CVM systematically reduces T_c by about a factor 0.7. We find a clear trend of increasing T_c with Mn concentration, which, however, saturates at concentrations above 20%. The dotted lines are a fit to an equation of the form $T_c=T_c^{max}[1-\exp(-x/\xi)]$, with $T_c^{max}=441$ K (617 K) and $\xi=0.08$ for the gap corrected case and using the CVM (MF). We can see that in spite of the different nature of the longest-range interactions beyond $R>3a$, the T_c does not significantly change by adding the gap correction. So, the longest-range interactions do not play such an important role after all. T_c's above room temperature are predicted for $x\geqslant 9\%$. For Mn concentrations as large as 20%, we found that even with the Sc d shift, the Mn-induced impurity bands are sufficiently broad to wipe out all evidence of a band gap. For 11% Mn, however, a gap

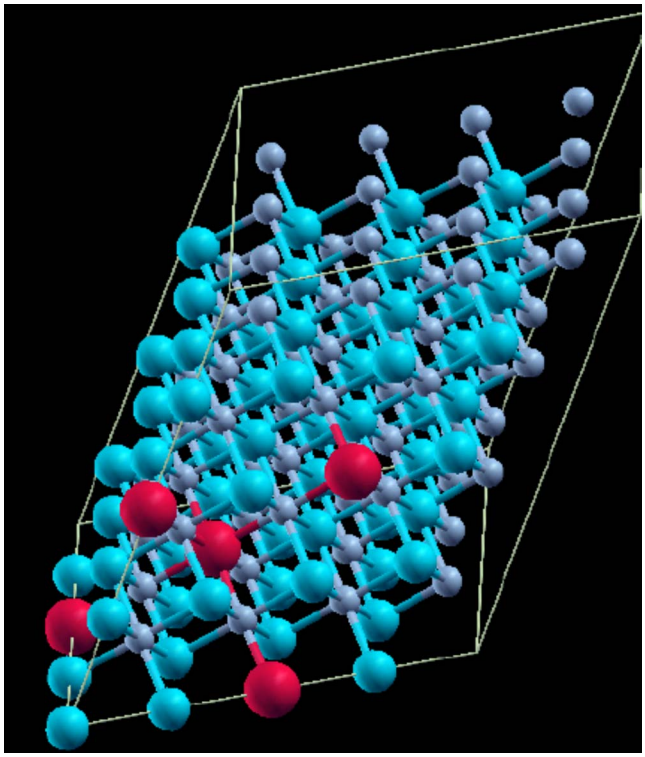

FIG. 5. (Color online) Structure of the 8% Mn-doped ScN 128 atom supercell, in which each Mn has a second nearest-neighbor Mn. Mn is shown in red (large spheres), Sc in light blue, and N in small silver spheres. Note the clustered aspect of the Mn containing region.

is still present, so we estimate that the gap closes at about 15%. Thus, above room temperature, a DMS in this system seems possible and even the higher concentration metallic systems may be useful magnetic materials because of the close lattice match of this system to GaN.

To gauge the relative importance of the second nearest-neighbor interaction, we note that the 64 atom cell with only one nearest-neighbor pair (6.25%) and no second nearest-neighbor pair had a $T_c^{MF}=296$ K and a $T_c^{CVM}=223$ K, which are somewhat smaller than the ones including a second nearest-neighbor pair. On the other hand, calculations for an 8% cell with all Mn placed as second nearest neighbors to each other had a lower T_c of only 209 K (MF) or 152 K (CVM). However, in this cell, Mn occurred in a pretty localized cluster, almost resembling a local MnN region, which is known to be antiferromagnetic, rather than a percolating chain of Mn second neighbor pairs. This interpretation is consistent with the magnetic exchange interactions for this case, as shown in Fig. 4.

D. Effects of carrier concentration and lattice constant

Next, we consider the effects of additional doping or defects affecting the carrier concentration. The easiest way to do this is by simply shifting the Fermi level, assuming a rigid band structure. This should be a good approximation for low doping levels. From the integrated density of states, we obtain the corresponding deviation of charge neutrality or carrier doping concentration. In Fig. 7 we show T_c^{MF} as a function of electron concentration. Positive values correspond to n-type doping and negative values to p-type doping. Interestingly, we can see that T_c drops for both p- and n-type doping with a maximum slightly above our charge neutrality point. The T_c stays relatively high up to about 1×10^{20} cm^{-3}, but then drops to about zero for about 3×10^{20} cm^{-3}. Such n-type carrier concentrations are rather typical of ScN samples, and this may be the reason why there has thus far been only one report of magnetism in this system.[3] It was, however, possible to reduce carrier concentrations in ScN to the 10^{17} cm^{-3} level.[24] For p-type doping (negative electron concentrations in Fig. 7) the T_c drops rather precipitously and we found this to lead to a spin-glass-like behavior. The

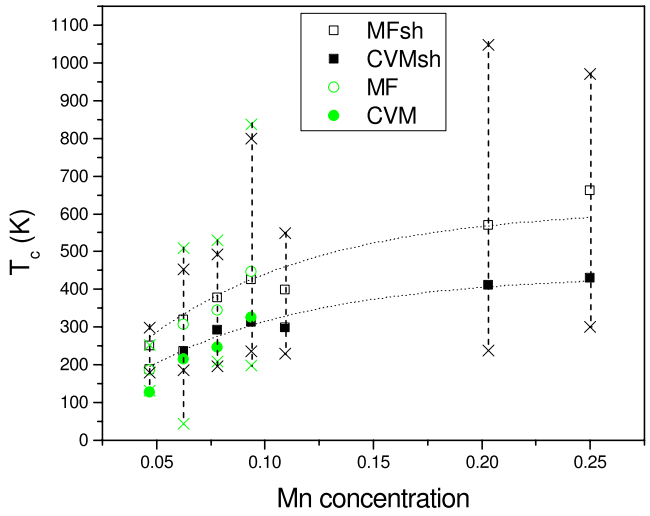

FIG. 6. (Color online) Mean-field (open symbols) and cluster variation method (filled) Curie temperatures for Mn-doped ScN as a function of Mn concentration: green circles, LDA; black squares, including gap correction. The × symbols indicate the range of the individual $J_i/3k_B$ on different atoms; in other words, the statistical fluctuation. Dotted lines are a fit to an exponential saturation curve as described in the text.

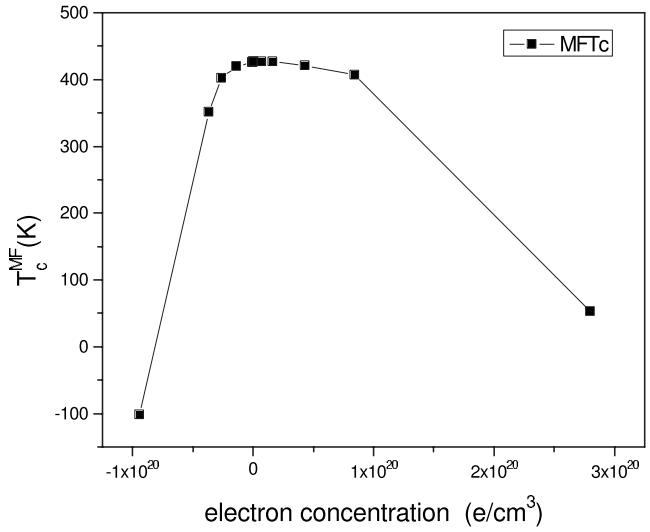

FIG. 7. Mean-field T_c as a function of electron concentration.

lowest spin wave frequencies in this case were found to be negative,[25] which indicates the instability of the ferromagnetic state for which we calculated the exchange interactions.

This unintentional background n-type doping in ScN is generally believed to originate from nitrogen vacancies. We have thus also carried out some simulations of cells with either 7.8% or 9.4% Mn and 3% V_N, i.e., two V_N per cell. The mean-field T_c was found to decrease by 4–14 %. These vacancy concentrations correspond to doping by about $6 \times 10^{19}\ e/\mathrm{cm}^3$, and the results are thus qualitatively consistent with the above rigid band results.

Finally, we note that Mn incorporation was found to shrink the lattice constant according to Vegard's law.[2] Including this effect on at least one concentration (8%) was found to increase the exchange interactions by ~15% and may thus further enhance T_c.

IV. CONCLUSIONS

In conclusion, linear response calculations show that Mn-doped ScN is a promising candidate DMS system with some unique properties. Most importantly, the solubility bottleneck is avoided because of the common crystal structure between ScN and MnN. Accurate calculations of the exchange interactions and the critical temperature indicate the possibility of above room temperature T_c for achievable Mn concentrations of the order of 10%. The doping study predicts that the key to achieve this goal is to keep the unintentional n-type carrier concentration below the $10^{20}\ \mathrm{cm}^{-3}$ level. This system is expected to be advantageous for spin lifetime because the spin-polarized electron carriers at the ScN conduction band minimum (at X) are expected to be less subjected to spin-orbit scattering than typical p-type DMS such as Mn-doped GaAs, because this would require intervalley scattering from one X point in the Brillouin zone to another.[26]

ACKNOWLEDGMENTS

The work at CWRU was supported by the Office of Naval Research under Grant No. N00014-02-1-0880 and the Army Research Office under Grant No. W911BF-06-1-0476. The work at UNL was supported by the Nebraska Research Initiative. The work at ASU was supported by the Office of Naval Research under Contract No. N00014-07-1-0479. Calculations were performed at the Ohio Supercomputer Center. We thank A. Ruban for providing the SQS generating program, and G. D. Samolyuk and V. P. Antropov for providing the CVM program and a preprint containing a description of this method. We also thank A. R. Smith for helpful discussions and C. Constantin for providing his Ph.D. thesis.

[1] A. Herwadkar and W. R. L. Lambrecht, Phys. Rev. B **72**, 235207 (2005).
[2] H. A. Al-Brithen, H. Yang, and A. R. Smith, J. Appl. Phys. **96**, 3787 (2004).
[3] At least one sample with 3% Mn was reported to show a ferromagnetic behavior up to at least 50 K in Costel Constantin, Ph.D. thesis, Ohio University, 2005.
[4] A. I. Liechtenstein, M. I. Katsnelson, V. P. Antropov, and V. A. Gubanov, J. Magn. Magn. Mater. **67**, 65 (1987).
[5] V. P. Antropov, M. I. Katsnelson, B. N. Harmon, M. van Schilfgaarde, and D. Kusnezov, Phys. Rev. B **54**, 1019 (1996).
[6] P. Hohenberg and W. Kohn, Phys. Rev. **136**, B864 (1964); W. Kohn and L. J. Sham, Phys. Rev. **140**, A1133 (1965).
[7] O. Gunnarsson and B. I. Lundqvist, Phys. Rev. B **13**, 4274 (1976).
[8] U. von Barth and L. Hedin, J. Phys. C **5**, 2064 (1972).
[9] O. K. Andersen, Phys. Rev. B **12**, 3060 (1972); O. K. Andersen, T. Saha-Dasgupta, R. W. Tank, C. Arcangeli, O. Jepsen, and G. Krier, in *Electronic Structure and Physical Properties of Solids, The Uses of the LMTO Method*, edited by H. Dreyssé, Lecture Notes in Physics (Springer, Berlin, 2000), p. 3.
[10] J. L. Xu, M. van Schilfgaarde, and G. D. Samolyuk, Phys. Rev. Lett. **94**, 097201 (2005).
[11] L. Bergqvist, O. Eriksson, J. Kudrnovský, V. Drchal, P. Korzhavyi, and I. Turek, Phys. Rev. Lett. **93**, 137202 (2004).
[12] G. D. Samolyuk and V. P. Antropov (unpublished).
[13] V. G. Vaks and G. D. Samolyuk, J. Exp. Theor. Phys. **88**, 89 (1999).
[14] H. E. Stanley, Phys. Rev. **179**, 570 (1963).
[15] We write the classical Heisenberg Hamiltonian as $H = -\Sigma_{i<j} J_{ij} \mathbf{e}_i \cdot \mathbf{e}_j$, i.e., counting each pair only once and in terms of unit vectors $\mathbf{e}_i$.
[16] P. Lloyd and P. V. Smith, Adv. Phys. **21**, 69 (1972).
[17] A. Zunger, S.-H. Wei, L. G. Ferreira, and J. E. Bernard, Phys. Rev. Lett. **65**, 353 (1990).
[18] A. V. Ruban, S. I. Simak, S. Shallcross, and H. L. Skriver, Phys. Rev. B **67**, 214302 (2003).
[19] M. Abramowitz and I. A. Stegun, *Handbook of Mathematical Functions* (Dover, New York, 1965), Chap. 10.2.
[20] M. A. Ruderman and C. Kittel, Phys. Rev. **96**, 99 (1954).
[21] T. Kasuya, Prog. Theor. Phys. **16**, 45 (1956).
[22] K. Yosida, Phys. Rev. **106**, 893 (1957).
[23] W. R. L. Lambrecht, Phys. Rev. B **62**, 13538 (2000).
[24] T. D. Moustakas, R. J. Molnar, and J. P. Dismukes, Proc.-Electrochem. Soc. **96**, 197 (1996).
[25] The spin wave frequencies are obtained from the secular equation $\det\{\omega(\mathbf{k})\delta_{ij}\frac{2}{\mu_i} - \frac{2}{\mu_i}[J_{ij}(\mathbf{k}) - \Sigma_k J_{ik}(0)\delta_{ij}]\frac{2}{\mu_j}\} = 0$.
[26] R. J. Elliott, Phys. Rev. **96**, 266 (1954).